RESEARCH ARTICLE | JULY 07 2023

Self-corrected orthonormalized ghost imaging through dynamic and complex scattering media ⊘

Lina Zhou ⬤ ; Yin Xiao ⬤ ; Wen Chen ✉ ⬤

Check for updates

⊕
View
Online

↱
Export
Citation

CrossMark

Self-corrected orthonormalized ghost imaging through dynamic and complex scattering media

View Online　　Export Citation　　CrossMark

Lina Zhou,[1] (iD) Yin Xiao,[1] (iD) and Wen Chen[1,2,a] (iD)

AFFILIATIONS

[1]Department of Electronic and Information Engineering, The Hong Kong Polytechnic University, Hong Kong, China
[2]Photonics Research Institute, The Hong Kong Polytechnic University, Hong Kong, China

[a]Author to whom correspondence should be addressed: owen.chen@polyu.edu.hk

ABSTRACT

In this Letter, we report a setup design to realize high-visibility orthonormalized ghost imaging (GI) with self-correction through dynamic and complex scattering media at low sampling ratios. With the design of a parallel detection, a mismatch between illumination patterns and intensity measurements is corrected. Gram–Schmidt orthonormalization is further applied to the illumination patterns and corrected intensities in order to implement high-visibility GI through dynamic and complex scattering media at low sampling ratios. It is experimentally demonstrated that the proposed self-correction and orthonormalization enable high-visibility and high-efficiency GI through dynamic and complex scattering media at low sampling ratios. The proposed method offers a promising alternative to overcome the challenge faced by conventional GI in implementing high-visibility object reconstruction through dynamic and complex scattering media at low sampling ratios.

Published under an exclusive license by AIP Publishing. https://doi.org/10.1063/5.0158244

Ghost imaging (GI)[1–5] using a single-pixel detector has emerged to be promising for indirect imaging. Compared to traditional imaging based on pixelated arrays [e.g., charge-coupled device (CCD)], GI requires only single-pixel detection for the measurements and object reconstruction. GI with single-pixel detectors could outperform those with pixelated arrays in some aspects, e.g., reliable endurance, fast response time, wide bandwidth, and high sensitivity.[6–9] Owing to these remarkable characteristics, GI has been proven to be a powerful complement to traditional imaging. With the development of spatial light modulator (SLM), spatial sampling is shifted to enable computational GI with new algorithms[10–13] (e.g., differential, normalized, and Gerchberg–Saxton-like). However, it could be time-consuming for GI to meet the demand of a large number of measurements for high-quality object reconstruction.

To address the aforementioned limitation, GI methods have been further developed to realize object reconstruction at low sampling ratios, e.g., orthogonal,[14–16] compressed sensing,[17] and neural networks.[18–20] Owing to the reduced sampling ratios, applications of GI have been extended to many fields,[21–26] e.g., microscope and photoacoustic. Although GI has been developed to implement object reconstruction, conventional GI cannot effectively reconstruct the object through dynamic and complex scattering media at low sampling ratios. This is ascribed to a consistency problem between illumination

patterns and intensity measurements, which is susceptible to dynamic scaling factors aroused by dynamic and complex scattering media. This inconsistency holds responsible for a failure of conventional GI through dynamic and complex scattering media. It is a challenge for current GI to implement high-visibility object reconstruction through dynamic and complex scattering media at low sampling ratios.

In this Letter, we report high-visibility self-corrected orthonormalized GI through dynamic and complex scattering media at low sampling ratios. A parallel detection with single-pixel detectors is first developed to correct a mismatch between illumination patterns and intensity measurements. This self-correction of dynamic scaling factors is fundamental and important for the development of GI through dynamic and complex scattering media. Gram–Schmidt orthonormalization is further applied to random illumination patterns and corrected intensities for the proposed GI through dynamic and complex scattering media at low sampling ratios. It is experimentally demonstrated that the developed self-correction and orthonormalization enable high-visibility GI through dynamic and complex scattering media at low sampling ratios. The proposed method has a potential to be applied in various scattering environments, e.g., static or dynamic scattering media.

A schematic experimental setup for the proposed GI through dynamic and complex scattering media is shown in Fig. 1. A 532.0-nm
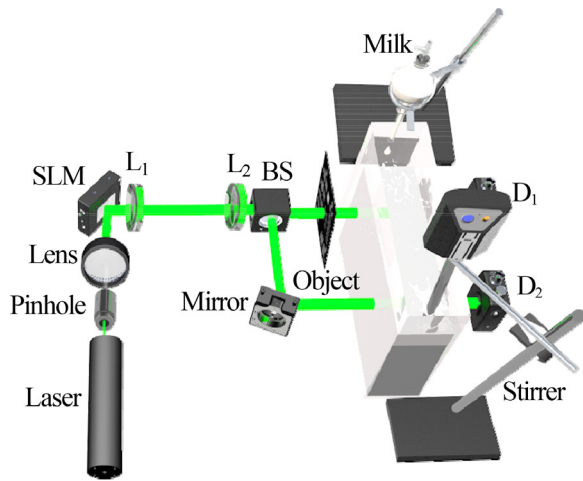
FIG. 1. A schematic setup for the proposed self-corrected orthonormalized GI through dynamic and complex scattering media at low sampling ratios. L_1 and L_2, focusing lenses with a focal length of 10.0 and 20.0 cm, respectively; D_1 and D_2, single-pixel bucket detectors; BS, beam splitter cube.

green laser (CrystaLaser, CL-2000) with a power of 25.0 mW is expanded and collimated to illuminate an amplitude-only SLM (Holoeye, LC-R720) with a pixel size of 20.0 μm. The random patterns with 128×128 pixels are sequentially embedded into SLM to modulate the optical wave. Then, the modulated wave propagates through a $4f$ optical system (i.e., L_1 with a focal length of 10.0 cm and L_2 with a focal length of 20.0 cm) before being projected onto an object. To implement the proposed GI through dynamic and complex scattering media, self-correction of dynamic scaling factors is first developed and conducted. This is realized by designing a parallel detection with two single-pixel detectors. A beam splitter cube is used to separate the propagating wave into reference wave and object wave. The dynamic and complex scattering media are generated by continuously dropping a certain volume of full cream milk into a transparent water tank [dimensions of 10.0 cm (L) $\times$ 30.0 cm (W) $\times$ 30.0 cm (H)], which contains 6000 ml of pure water. It is worth noting that full cream milk is directly added into a funnel, which initially contains 1000 ml of pure water. To generate dynamic and complex scattering media, a stirrer with a maximum speed of 1200 revolutions per minute (rpm) is applied. Single-pixel detectors (Thorlabs, PDA100A2) are placed to record light intensities. For synchronous measurements, a purpose-built Labview program is designed to synchronize and control the SLM and a data acquisition device (Smacq, USB-5210) connected with single-pixel detectors. Finally, dynamic scaling factors can be effectively corrected to enable high-visibility self-corrected orthonormalized GI through dynamic and complex scattering media at low sampling ratios.

Figure 2 shows a flow chart for the proposed GI through dynamic and complex scattering media at low sampling ratios. A series of random illumination patterns P_i are generated by

$$\sum P_i = cons,$$
$$= FT\{P_i\}_{(0,0)}, \tag{1}$$

where *cons* denotes the sum of pixel values of each illumination pattern and FT denotes Fourier transform. Light intensities B_i and B_{ir}
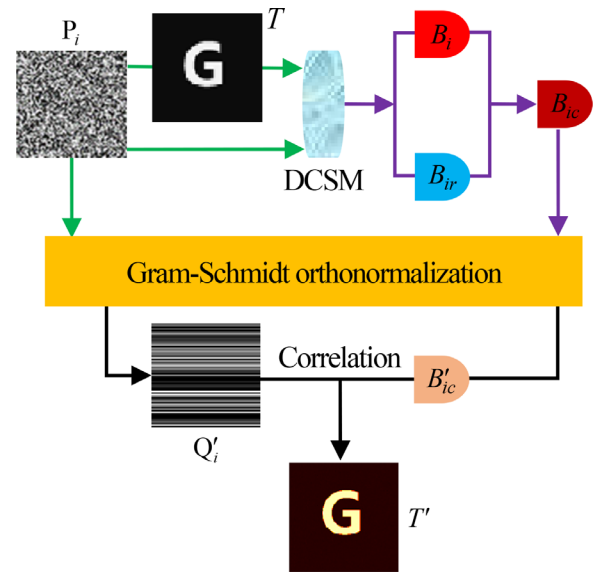

FIG. 2. A schematic for the proposed GI through dynamic and complex scattering media at low sampling ratios. P_i, the *i*th illumination pattern; T, an object; DCSM, dynamic and complex scattering media; B_i and B_{ir}, single-pixel intensity, respectively, recorded in object and reference wave paths with the *i*th illumination pattern P_i; B_{ic}, the *i*th corrected single-pixel value corresponding to the illumination pattern P_i; Q'_i, the *i*th orthonormalized pattern corresponding to the *i*th illumination pattern P_i; B'_{ic}, the *i*th orthonormalized single-pixel intensity corresponding to B_{ic}; T', a reconstructed object.

recorded by single-pixel detectors in object and reference wave paths can be, respectively, described by

$$B_i = k_i \sum P_i T, \tag{2}$$
$$B_{ir} = \tilde{k}_{ir} \sum P_i, \tag{3}$$

where T denotes an object and k_i and $\tilde{k}_{ir}$, respectively, denote a scaling factor aroused by dynamic and complex scattering media in the object and reference wave paths. Owing to dynamic scattering, the scaling factor is varied. There is no doubt that dynamic scaling factors result in a failure of conventional GI. Hence, the developed self-correction of dynamic scaling factors is necessary. For the proposed GI through dynamic and complex scattering media, there is a reasonable assumption given by

$$\tilde{k}_{ir} \approx k_i. \tag{4}$$

By applying Eq. (4), a corrected single-pixel intensity B_{ic} corresponding to P_i is obtained by

$$B_{ic} = \frac{B_i}{B_{ir}}. \tag{5}$$

Gram–Schmidt orthonormalization is further studied to implement high-visibility and high-efficiency GI through dynamic and complex scattering media at low sampling ratios, as shown in Fig. 2. The illumination pattern P_i is first reshaped to a one-dimensional vector R_i. Then, a series of one-dimensional orthogonal vectors Q_i are obtained by

$$Q_1 = R_1,$$
$$Q_2 = R_2 - C_{21}Q_1,$$
$$Q_3 = R_3 - C_{31}Q_1 - C_{32}Q_2,$$
$$\vdots$$
$$Q_i = R_i - \sum_{j=1}^{i-1} C_{ij}Q_j, \tag{6}$$

where j denotes an integer ranging from 1 to $i - 1$ and C_{ij} denotes a projection coefficient described by

$$C_{ij} = \frac{R_i \bullet Q_j}{Q_j \bullet Q_j}, \tag{7}$$

where $\bullet$ denotes an inner product of two one-dimensional vectors. When big values exist in orthogonal vectors Q_i, orthogonal vectors can be further normalized[16] as described by

$$\tilde{Q}_i = \frac{Q_i}{\|Q_i\|}, \tag{8}$$

where $\|\|$ denotes a L_2-norm operation. To maintain a relationship between orthonormalized patterns $\tilde{Q}_i$ and corrected intensities B_{ic}, B_{ic} is also orthonormalized as described by

$$\tilde{B}_{ic} = B_{ic} - \sum_{j=1}^{i-1} C_{ij}\tilde{B}_{jc}, \tag{9}$$

$$B'_{ic} = \frac{\tilde{B}_{ic}}{\|Q_i\|}. \tag{10}$$

One-dimensional orthonormalized vector $\tilde{Q}_i$ should be reshaped to 2D pattern Q'_i for object reconstruction. With the rectified parameters of orthonormalized patterns Q'_i and intensities B'_{ic}, high-visibility GI through dynamic and complex scattering media at low sampling ratios can be realized as described by

$$T' = \frac{1}{N}\sum_{i=1}^{N} Q'_i\left(B'_{ic} - \langle B'_{ic}\rangle\right) = \langle Q'_i B'_{ic}\rangle - \langle Q'_i\rangle\langle B'_{ic}\rangle, \tag{11}$$

where T' denotes a reconstructed object image and $\langle\rangle$ denotes an ensemble average over the total number of measurements (i.e., N). By applying Eq. (11), high-visibility objects can be reconstructed in various complex environments at low sampling ratios.

Figures 3(a)–3(u) show the reconstructed objects using conventional GI, self-corrected GI, and the proposed method with the developed self-correction and orthonormalization, when the different number of realizations is used. A dynamic and complex scattering environment is generated by continuously dropping 5.0 ml full cream milk into water tank with a stirrer at 700.0 rpm. As can be seen in Figs. 3(a)–3(g), conventional GI cannot recover any effective information of the unknown object through dynamic and complex scattering media. GI with only the developed self-correction can work for imaging through dynamic and complex scattering media, and visibility of the reconstructed objects can be enhanced with more measurements as shown in Figs. 3(h)–3(n). However, a large number of measurements could impose a heavy burden on data acquisition, reducing the efficiency of self-corrected GI through dynamic and complex scattering
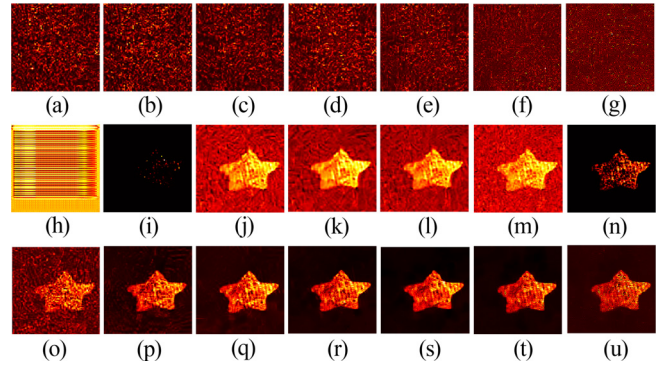

FIG. 3. The reconstructed object (128 × 128 pixels) obtained by using GI through dynamic and complex scattering media with the different number of measurements (2000 to 14 000 with an interval of 2000). (a)–(g) Reconstructed objects using conventional GI, (h)–(n) reconstructed objects using GI with only the developed self-correction, and (o)–(u) reconstructed objects using GI with the developed self-correction and orthonormalization.

media. GI with the developed self-correction and orthonormalization is studied to recover the object through dynamic and complex scattering media, as shown in Figs. 3(o)–3(u). With only 2000 measurements (i.e., a sampling ratio of 12.2%) collected by each single-pixel detector, the proposed method recovers effective information of the unknown object. When the number of measurements increases from 2000 to 14 000 with an interval of 2000 (i.e., sampling ratios of 12.2%, 24.4%, 36.6%, 48.8%, 61.0%, 73.2%, and 85.4%), the recovered object is of higher visibility. Furthermore, visibility of the reconstructed objects is much higher than that of reconstructed objects using GI with only the developed self-correction. Figure 3(p) shows that the proposed method is effective in recovering a high-visibility object with only 4000 measurements. It is experimentally verified that the developed self-correction and orthonormalization enable high-visibility and high-efficiency GI through dynamic and complex scattering media at low sampling ratios.

In Figs. 4(a) and 4(b), visibility[27] and SNR[28] are calculated to quantify the quality of recovered objects using conventional GI, self-corrected GI, and GI with the developed self-correction and orthonormalization. In conventional GI, visibility of reconstructed objects remains ~0. It is illustrated that conventional GI cannot work in dynamic and complex scattering media. With the developed self-correction used in GI (i.e., self-corrected GI), visibility of reconstructed objects can increase with more measurements. When the number of measurements collected by each single-pixel detector is 14 000, the visibility approaches 0.25. To recover the object with high-visibility, a large number of measurements are required in this case, which could prevent its applications. The developed self-correction and orthonormalization provide a promising approach for high-visibility and high-efficiency GI through dynamic and complex scattering media. Visibility of the reconstructed objects reaches 0.3 with only 2000 measurements collected by each single-pixel detector. Similarly, image quality can also be evaluated using SNR, as shown in Fig. 4(b). As can be seen in Fig. 4(b), SNR values of the retrieved images in conventional GI are always close to 0. In contrast, SNR values of the retrieved objects in the proposed method increase sharply as the number of measurements increases, and the SNR value can achieve to 5.7. SNR
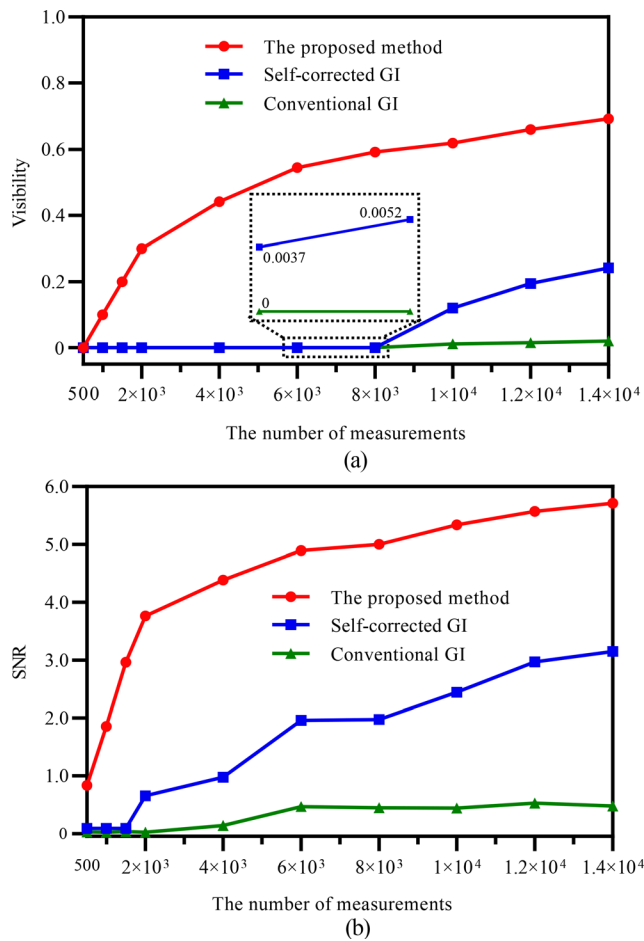
FIG. 4. (a) Visibility and (b) signal-to-noise ratio (SNR) of reconstructed objects obtained by conventional GI, GI with only the developed self-correction, and GI with the developed self-correction and orthonormalization in dynamic and complex scattering environments using the different number of measurements collected by each single-pixel detector.

values of the recovered objects using only the self-corrected GI can progressively enhance. However, SNR value of the recovered object using only the self-corrected GI is much lower than that obtained by using the proposed self-corrected orthonormalized GI when the same number of measurements is used. The operation of Gram–Schmidt orthonormalization can make random patterns orthogonal to each other and enhance independence of pixels. The low correlation among orthogonal patterns ensures that object information obtained from the samplings is of high-quality, effectively enhancing the sampling efficiency. The quantitative demonstration provides evidence that the proposed high-visibility and high-efficiency GI through dynamic and complex scattering media is feasible and effective.

In practice, scattering media could also exist between illumination source and the object. In a typical GI setup,[9] the reference beam is directed toward a CCD camera, while another beam is directed toward the object. When the diffuser is rotated, speckle pattern is recorded by

the CCD and deemed as the illumination pattern for correlation. A change of scattering media between illumination source and the object can be considered as a rotation of the diffuser to obtain different illumination patterns. When complex and dynamic scattering media also exist between illumination source and the object, speckle patterns can be recorded by using a CCD. Hence, the proposed self-corrected orthonormalized GI is also feasible and effective, when complex scattering media further exist between illumination source and the object. Here, there are scattering media between the object and the detector. Moreover, complex scattering media change over time. The scaling factor aroused by dynamic and complex scattering media changes over time. Hence, it severely affects the consistency between illumination patterns and collected light intensities, resulting in a failure of conventional GI. To overcome this challenge, self-corrected orthonormalized GI is proposed to implement effective and high-visibility imaging through dynamic and complex scattering media at low sampling ratios.

In conclusion, we have reported a setup design for high-visibility and high-efficiency GI through dynamic and complex scattering media at low sampling ratios. The developed self-correction of dynamic scaling factors using a parallel detection lays a good foundation for GI through dynamic and complex scattering media. Experimental results demonstrate that the developed self-correction and orthonormalization enable high-visibility and high-efficiency GI through dynamic and complex scattering media at low sampling ratios (e.g., 12.2%). The proposed method is applicable for high-visibility and high-efficiency object reconstruction in various complex environments, including static and dynamic scattering media. Typical examples are ground diffusers, smoke, fog, biological tissues, and turbid water. The proposed method aims to address the challenges posed by these scattering environments and achieve effective object reconstruction even at low sampling ratios. Its capability of object reconstruction through various scattering media at low sampling ratios illustrates its applicability in real-world scenarios. It is expected that the proposed method could stimulate the interest in further developments of GI through dynamic and complex scattering media at low sampling ratios.

AUTHOR DECLARATIONS
Conflict of Interest

The authors have no conflicts to disclose.

Author Contributions

Lina Zhou: Conceptualization (lead); Investigation (lead); Writing – original draft (lead). **Yin Xiao:** Investigation (supporting). **Wen Chen:** Conceptualization (lead); Methodology (lead); Supervision (lead); Writing – review & editing (lead).

DATA AVAILABILITY

The data that support the findings of this study are available from the corresponding author upon reasonable request.

REFERENCES

[1] W. L. Chan, K. Charan, D. Takhar, K. F. Kelly, R. G. Baraniuk, and D. M. Mittleman, Appl. Phys. Lett. **93**, 121105 (2008).

[2] A. V. Belinskii and D. N. Klyshko, Sov. Phys. JETP **78**, 259 (1994).

[3] T. B. Pittman, Y. H. Shih, D. V. Strekalov, and A. V. Sergienko, Phys. Rev. A **52**, R3429 (1995).

[4] D. V. Strekalov, A. V. Sergienko, D. N. Klyshko, and Y. H. Shih, Phys. Rev. Lett. **74**, 3600 (1995).

[5] A. Gatti, E. Brambilla, M. Bache, and L. A. Lugiato, Phys. Rev. Lett. **93**, 093602 (2004).

[6] S. Li, F. Cropp, K. Kabra, T. J. Lane, G. Wetzstein, P. Musumeci, and D. Ratner, Phys. Rev. Lett. **121**, 114801 (2018).

[7] M. Sun, M. P. Edgar, G. M. Gibson, B. Sun, N. Radwell, R. Lamb, and M. J. Padgett, Nat. Commun. **7**, 12010 (2016).

[8] D. Pelliccia, A. Rack, M. Scheel, V. Cantelli, and D. M. Paganin, Phys. Rev. Lett. **117**, 113902 (2016).

[9] Y. Bromberg, O. Katz, and Y. Silberberg, Phys. Rev. A **79**, 053840 (2009).

[10] J. H. Shapiro, Phys. Rev. A **78**, 061802 (2008).

[11] F. Ferri, D. Magatti, L. A. Lugiato, and A. Gatti, Phys. Rev. Lett. **104**, 253603 (2010).

[12] B. Sun, S. S. Welsh, M. P. Edgar, J. H. Shapiro, and M. J. Padgett, Opt. Express **20**, 16892 (2012).

[13] W. Wang, X. Hu, J. Liu, S. Zhang, J. Suo, and G. Situ, Opt. Express **23**, 28416 (2015).

[14] L. Wang and S. Zhao, Photonics Res. **4**, 240 (2016).

[15] H. Yu, R. Lu, S. Han, H. Xie, G. Du, T. Xiao, and D. Zhu, Phys. Rev. Lett. **117**, 113901 (2016).

[16] B. Luo, P. Yin, L. Yin, G. Wu, and H. Guo, Opt. Express **26**, 23093 (2018).

[17] O. Katz, Y. Bromberg, and Y. Silberberg, Appl. Phys. Lett. **95**, 131110 (2009).

[18] G. M. Gibson, S. D. Johnson, and M. J. Padgett, Opt. Express **28**, 28190 (2020).

[19] N. Radwell, S. D. Johnson, M. P. Edgar, C. F. Higham, R. Murray-Smith, and M. J. Padgett, Appl. Phys. Lett. **115**, 231101 (2019).

[20] Z. Ye, D. Sheng, Z. Hao, H. B. Wang, J. Xiong, X. Wang, and W. Jin, Appl. Phys. Lett. **117**, 091103 (2020).

[21] N. D. Hardy and J. H. Shapiro, Phys. Rev. A **84**, 063824 (2011).

[22] N. Radwell, K. J. Mitchell, G. M. Gibson, M. P. Edgar, R. Bowman, and M. J. Padgett, Optica **1**, 285 (2014).

[23] R. I. Stantchev, X. Yu, T. Blu, and E. Pickwell-MacPherson, Nat. Commun. **11**, 2535 (2020).

[24] B. Sun, M. P. Edgar, R. Bowman, L. E. Vittert, S. Welsh, A. Bowman, and M. J. Padgett, Science **340**, 844 (2013).

[25] R. E. Meyers, K. S. Deacon, and Y. Shih, Appl. Phys. Lett. **98**, 111115 (2011).

[26] H. Li, J. Shi, Y. Zhu, and G. Zeng, Appl. Phys. Lett. **103**, 051901 (2013).

[27] R. I. Khakimov, B. M. Henson, D. K. Shin, S. S. Hodgman, R. G. Dall, K. G. H. Baldwin, and A. G. Truscott, Nature **540**, 100 (2016).

[28] B. Redding, M. A. Choma, and H. Cao, Nat. Photonics **6**, 355 (2012).